Comparison of Terrain Following and Cut Cell Grids with a Non-Hydrostatic Model

JAMES SHAW*

ABSTRACT

Enter the text of your abstract here.

TODO: *Builds on the work of Schär et al. (2002), Klemp (2011), Weller and Shahrokhi (2014) (all MWR)*
Results also compared with Melvin et al. (2010) (QRJ), maybe zaengl2012 (MWR), Good et al. (2014) (Atmos Sci Letters)

you can do better than this on the motivation. I have put on dropbox for you the motivational papers that I cited in my curl free pressure gradients paper

1. Introduction

Representing orography accurately in numerical weather prediction systems is necessary to model downslope winds and local precipitation patterns. There are two main approaches to represent orography on a grid: terrain following layers and cut cells. Both methods align cells in vertical columns.

With terrain following (TF) layers the terrain's influence decays with height so that the bottommost layers follow the underlying surface closely while the uppermost layers are flat. TF layers are usually implemented on a rectangular computational grid using transformed coordinates.

It is well-known that TF coordinates perform badly in the presence of steep orography: as model resolution increases, steeper gradients lead to larger truncation errors in calculating the horizontal pressure gradient which result in spurious winds (Dempsey and Davis 1998; Steppeler et al. 2002).

Much work has been done to reduce error associated with TF coordinates: firstly by smoothing the effects of terrain with height (Schär et al. 2002; **?**; Klemp 2011) and, secondly, by improving the accuracy in calculating the horizontal pressure gradient itself (Klemp 2011; Zängl 2012).

Despite their associated numerical errors, TF coordinates are attractive because their rectangular structure is simple to process by computer, boundary layer resolution can be increased with variable spacing of vertical layers (Schär et al. 2002), and cell sizes remain almost constant (Jebens et al. 2011).

Cut cells is an alternative method in which cells that lie entirely below the terrain are removed, and those that intersect the surface are modified in shape so that they more closely fit the terrain. This modification means that some cells become very small, which can reduce computational efficiency (Klein et al. 2009), and several approaches have been tried to alleviate the problem (Steppeler et al. 2002; Yamazaki and Satomura 2010; Jebens et al. 2011).

Several studies have found that cut cells produce more accurate results when compared to TF coordinates. Spurious winds seen in TF coordinates are not present and errors do not increase with steeper terrain (Good et al. 2014). A comparison of TF and cut cells using real initial data by Steppeler et al. (2006) found that precipitation patterns, temperature and wind fields were forecast more accurately in the cut cell model.

although the TF model was later improved, removing the advantage of cut cells

Many comparisons of TF and cut cell grids have made between different models. On the contrary, this study uses the nonhydrostatic model from Weller and Shahrokhi (2014) to enable a like-for-like comparison between BTF, SLEVE and cut cell grids for idealised, two-dimensional test cases from the literature. TODO: *final bit of intro: in section 2, section 3 etc etc*

TODO: *TF grids often shown to have lesser accuracy than cut cells in some test cases, often significantly so. Our results demonstrate that accuracy need not be much reduced and can even be better than cut cells.*

2. Grids

TODO: *introduce this section* Gal-Chen and Somerville (1975) proposed a basic terrain following (BTF) coordinate defined as

$$z = (H - h)\,(z^\star / H) + h \tag{1}$$

where, in two dimensions, $z(x, z^\star)$ is the height of the coordinate surface at level $z^\star$, H is the height of the domain,

*Corresponding author address: Dept., Institution, Address, City, State/Country.
E-mail: j.shaw@pgr.reading.ac.uk

Further motivation:
Previous comparisons have been made with models without curl free pressure gradients. Most operational models remain TF. Should they be changing to cut cells? A like for like comparison and a new test case which exposes problems with cut cells

and $h(x)$ is the height of the terrain surface. Using this coordinate, the terrain's influence decays linearly with height but disappears only at the top of the domain.

The sigma coordinate transform of Phillips (1957) is equivalent to the BTF coordinate transform since they both decay linearly. However, since they decay with pressure rather than height, sigma coordinates also change with horizontal variations in pressure.

The smooth level vertical (SLEVE) coordinate proposed by Schär et al. (2002) achieves a more regular TF grid in the middle and top of the domain than the BTF coordinate. The terrain height is split into large-scale and small-scale components, h_1 and h_2, such that $h = h_1 + h_2$, with each component having a different exponential decay. The transformation is defined as

$$z = z^\star + h_1 b_1 + h_2 b_2 \tag{2}$$

where the vertical decay functions are given by

$$b_i = \frac{\sinh\left((H/s_i)^n - (z^\star/s_i)^n\right)}{\sinh\left(H/s_i\right)^n} \tag{3}$$

with s_1 and s_2 are the scale heights of large-scale and small-scale terrain respectively. The exponent n was introduced by Leuenberger et al. (2010) in order to increase cell thickness in the layers nearest the ground, allowing longer timesteps and permitting more accurate calculation of parameterised low-level heat and momentum fluxes. Leuenberger et al. (2010) found the exponent has an optimal value of $n = 1.35$. Choosing $n = 1$ gives the decay functions used by Schär et al. (2002).

TODO: *Explain how SnapCol grid is constructed?*

3. Results

A series of standard, two-dimensional tests were performed over idealised orography. For each test, results on the BTF, SLEVE and cut cell grid are compared. We use a finite volume discretisation of the fully-compressible Euler equations described by Weller and Shahrokhi (2014). The model has a curl-free pressure gradient formulation, an upwind-biased cubic advection scheme, and uses a Lorenz staggering of thermodynamic variables. No explicit diffusion is used in any of the tests.

a. Advection

Following Schär et al. (2002), a tracer is transported above wave-shaped terrain by solving the advection equation for a prescribed horizontal wind. This challenges the accuracy of the advection scheme in the presence of grid distortions. The spatial domain, terrain profile, wind field, tracer, SLEVE scale heights are given by Schär et al. (2002). The optimisation of SLEVE by Leuenberger et al. (2010) is not used, so the exponent $n = 1$. A tracer is placed above and to the left of the mountain with a magnitude of 1 at its centre and 0 at the perimeter.

While the continuous wind field specified by Schär et al. (2002) is non-divergent, this is not true of the discrete wind field on non-orthogonal grids. A potential, p, is used to correct the wind field, $\boldsymbol{u}$, so that is non-divergent such that

You haven't fully described the projection method or said that it is a projection method

$$\nabla \cdot (\boldsymbol{u} + \nabla p) = 0, \tag{4}$$

which can be rearranged to give a Poisson equation

$$\nabla^2 p = -\nabla \cdot \boldsymbol{u}. \tag{5}$$

The flux form of the advection equation, $\partial\phi/\partial t + \nabla \cdot (\boldsymbol{u}\phi) = 0$, is solved using an upwind-biased cubic advection scheme which is non-monotonic and not flux corrected. The time derivative is solved using a second order Runge-Kutta scheme. TODO: *I ought to understand this method myself!*

Unlike Schär et al. (2002) who use periodic lateral boundaries, a fixed value of 0 is used at the inlet boundary and all other boundaries have zero gradient. Tests are integrated forward in time for 10 000 s with a timestep of $\Delta t = 25$ s.

The test was executed on the BTF, SLEVE and cut cell grids, and on a regular grid with flat terrain. Tracer contours at $t = 0$ s, 5000 s and 10 000 s are shown in Figure 1. The result from Schär et al. (2002) using a fourth-order centred scheme and sigma coordinates (1a) is compared with the upwind-biased cubic scheme on (1b) the BTF grid, and (1c) cut cell grid.

Tracer magnitude and shape are well-preserved on all grids, both above the mountain at $t = 5000$ s and past the mountain at $t = 10\,000$ s. Advection is most accurate on the cut cell grid (figure 1c) and regular grid (not shown). As found by Good et al. (2014), the result is the same on both grids. This is to be expected since the wind is zero in the region of the ground and both grids are orthogonal elsewhere. On the BTF grid, the tracer is less distorted by the cubic upwind-biased scheme (figure 1b) compared to the fourth-order centred scheme from Schär et al. (2002) (figure 1a).

Minimum and maximum tracer values and ℓ^2 error norms on the BTF, SLEVE, cut cell and regular grids are summarised in table 1. The results of the cubic upwind-biased scheme on TF and regular grids are comparable with those for the fourth-order centred scheme from Schär et al. (2002). Error is largest on the BTF grid with $\ell^2 = 0.007\,58$ but significant reduced on the SLEVE grid with $\ell^2 = 0.001\,10$. The error is approximately halved by changing from the SLEVE grid to the cut cell grid.

The results of the tracer advection test show that, given an advection scheme of a sufficiently high order, distortions in the grid do not significantly distort the tracer.

even on the very distorted BTF grid

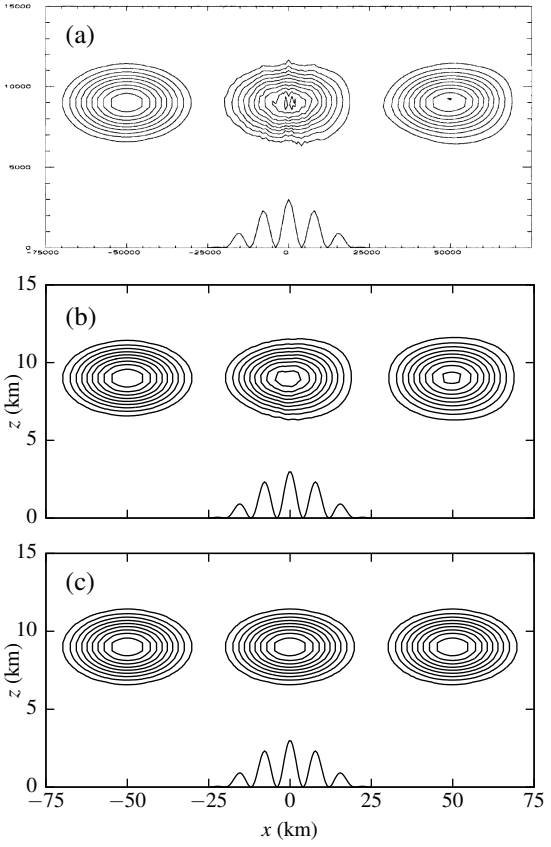

I think you should say that schar et all use the BTF grid

FIG. 1. Horizontally advected tracer contours at $t = 0$ s, 5000 s and 10000 s using (a) the fourth-order centred difference scheme with sigma coordinates from Schär et al. (2002), and the upwind-biased cubic scheme on (b) BTF grid, (c) cut cell grid. Contour intervals are every 0.1.

TABLE 1. Minimum and maximum tracer magnitudes and ℓ^2 error norms at $t = 10000$ s in the tracer advection test. Results of the cubic upwind-biased scheme are compared with the fourth-order centred scheme from Schär et al. (2002).

	Cubic upwind-biased			Schär 4th order	
	ℓ^2 error	min	max	min	max
Analytic	0	0	1	0	1
BTF	0.00758	−0.034	0.928	−0.058	1.001
SLEVE	0.00110	−0.011	0.981	−0.002	0.984
Cut cell	0.00058	−0.007	0.982	—	—
No orography	0.00058	−0.007	0.982	−0.002	0.984

b. *Resting atmosphere*

resting

An idealised terrain profile is defined along with a stratified atmosphere in hydrostatic balance. The analytic solution is time-invariant, but numerical errors in calculating the horizontal pressure gradient can give rise to spurious velocities which become more severe over steeper terrain

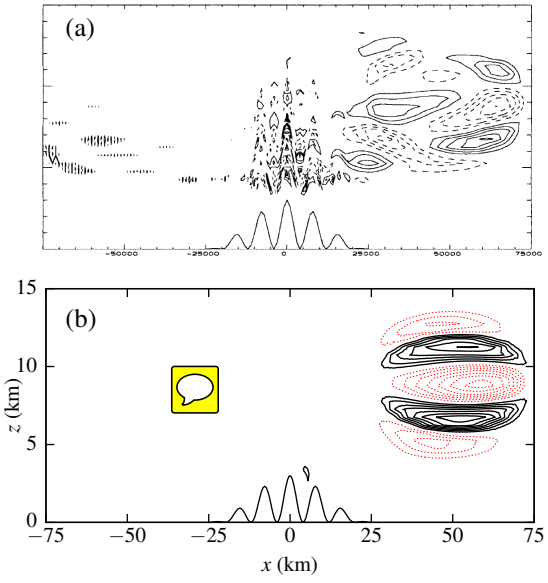

FIG. 2. Errors in horizontal tracer advection at $t = 10000$ s using (a) the fourth-order centred difference scheme with sigma coordinates from Schär et al. (2002), (b) the upwind-biased cubic scheme on a BTF grid. Contour intervals are every 0.01 with negative contours denoted by dashed lines.

Klemp (2011). The test setup follows the specification by Klemp (2011) but uses the smaller domain and rigid boundaries from Weller and Shahrokhi (2014).

The test was integrated forward by 5 hours on the BTF, SLEVE and cut cell grids, and a regular grid with flat terrain. Maximum vertical velocities are compared with the results from Klemp (2011) in figure 3 (note different vertical scales). In agreement with Klemp (2011), vertical velocities are larger on more distorted grids. However, magnitudes are smaller comparing results on the terrain following grids with those from Klemp (2011), with w reaching a maximum of $\sim 0.35\,\mathrm{m\,s^{-1}}$ on the BTF grid in our test compared with a maximum of $\sim 10\,\mathrm{m\,s^{-1}}$ found by Klemp (2011).

Unlike the result from Klemp (2011), the SLEVE grid does not significantly reduce vertical velocities compared to the BTF grid. However, errors are three orders of magnitude smaller on the cut cell grid with vertical velocities of $\sim 1\times10^{-3}\,\mathrm{m\,s^{-1}}$. The smallest error of $\sim 1\times10^{-10}\,\mathrm{m\,s^{-1}}$ is found on the regular grid.

Good et al. (2014) found the maximum vertical velocity in their cut cell model was $1\times10^{-12}\,\mathrm{m\,s^{-1}}$, which is better than any result obtained using the model by Weller and Shahrokhi (2014). It is worth noting that Good et al. (2014) used a timestep of 1.01 s instead of the 100 s timestep specified by Klemp (2011) that was used to obtain the results presented here. In addition, in the model used by Good et al. (2014), cell centres are in the centre of the uncut cell, resulting in the centre of some cut cells

I don't think the time step will make much of a difference. But you could check this. They just needed a very small time step because acoustic waves were treated explicitly

being below the ground (S.-J. Lock 2014, personal communication). This means that the grid is effectively regular when calculating horizontal and vertical gradients. These two modelling decisions may account for the very small velocities found by Good et al. (2014).

In summary, spurious velocities in the resting atmosphere test were similar on both terrain following grids, with much lower errors compared to those from Klemp (2011). The maximum vertical velocity was significantly decreased on the cut cell grid, so we conclude that non-orthogonality is a significant cause of numerical error in this test. Non-orthogonality is not necessarily the problem. Grid alignment with the stratification will be very important for this test case

c. Gravity waves

- TODO: *Motivation: it models a real dynamic process?* Flow that interacts with the orography
- Specify domain, thermodynamics, prescribed inlet wind
- Specify sponge layers, BCs
- Compare BTF, SLEVE and SnapCol results (SLEVE only briefly as visually identical to BTF)

Analysis:

- w contours visually similar on all grids, agree with Melvin et al. (2010) (Figure 4)
- TODO: *divergence might help explain computational mode – it's greater on the SnapCol grid (MSc dissertation Figure 4.15e)*
- θ anomalies similar on all grids EXCEPT...
- ... on SnapCol grid in lee of mountain near the ground. (Figure 5)
- TODO: *worth mentioning implications of this? 1. reduced stability, although not enough to create vertical motion in this instance 2. would disrupt clouds 2. model has no viscosity so thermal mixing should not occur in theory*
- Lorenz computation mode has been excited because Exner sample line at $x = 50$km is in hydrostatic balance (Figure 6)
- TODO: *We can speculate on what excites the computational mode, but perhaps better not to?*
- No evidence of small cell problem – TODO: *don't know that we can say much here without another vertical momentum test; our hypothesis about the quasi-horizontal flow isn't backed up with a test case*
- Conclusion: results similar on all grids, agree with literature, except for Lorenz computational mode on SnapCol grid

are these plots done with gnuplot?

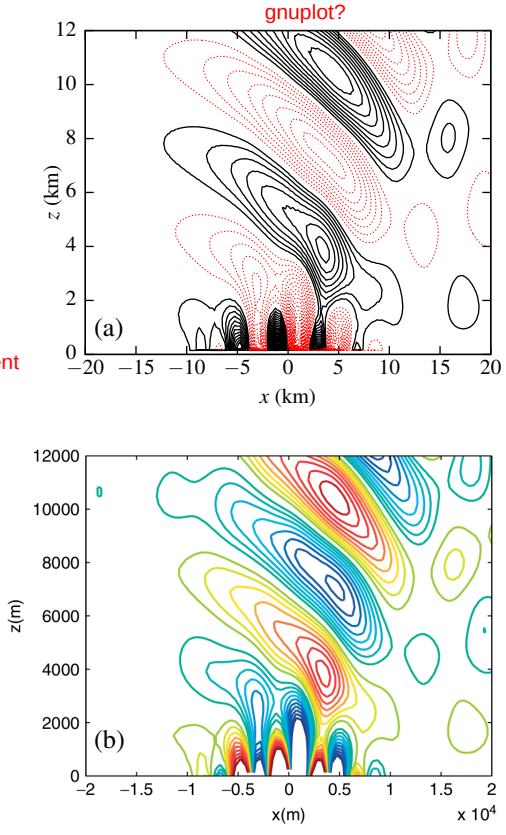

FIG. 4. Vertical cross section of vertical velocity contours in the gravity waves test after 5 hours on (a) the BTF grid compared with (b) the mass-conserving semi-implicit semi-Lagrangian solution from Melvin et al. (2010). Contours are every 5×10^{-2} m s^{-1} with solid lines denoting ascent and dashed lines descent.

4. Conclusions

1. BTF grid isn't as bad as people say it is. We found that:
   - Upwind-biased cubic advection scheme accurately advects a tracer in non-divergent flows (Figure 1, 2, Table 1)
   - spurious vertical velocities are small in resting atmosphere (Figure 3)
   - gravity waves results visually as good as reference solution from Melvin et al. (2010) (figure 4)
2. Cut cell grids can be worse than TF grids:
   - Lorenz computational mode found on SnapCol grid only (figure 5, 6)
3. Cut cell grids can also be better than TF grids in more artificial test cases:

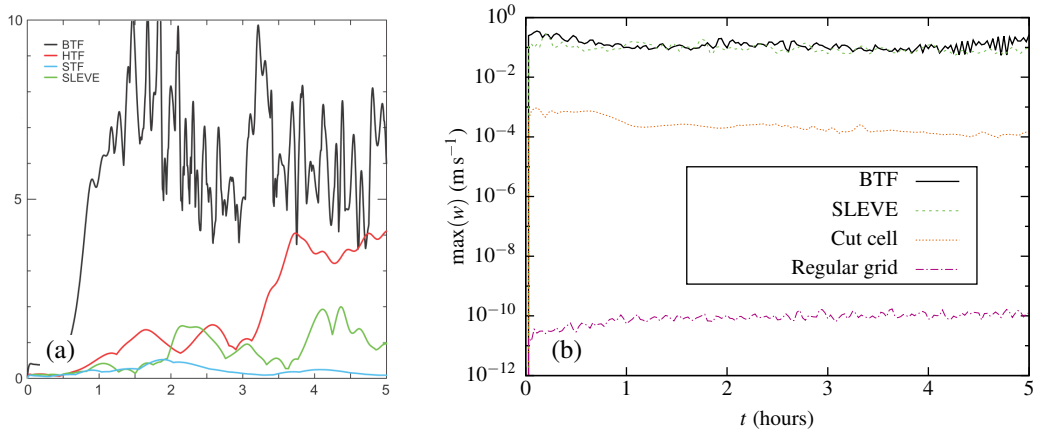

FIG. 3. Maximum spurious vertical velocity, w ($\mathrm{m\,s^{-1}}$), in the resting atmosphere test with results on (a) BTF, SLEVE, Hybrid Terrain Following (HTF) and Smoothed Terrain Following (STF) coordinates from Klemp (2011), (b) BTF, SLEVE, cut cell and regular grids using the model from Weller and Shahrokhi (2014). Note that vertical scales differ.

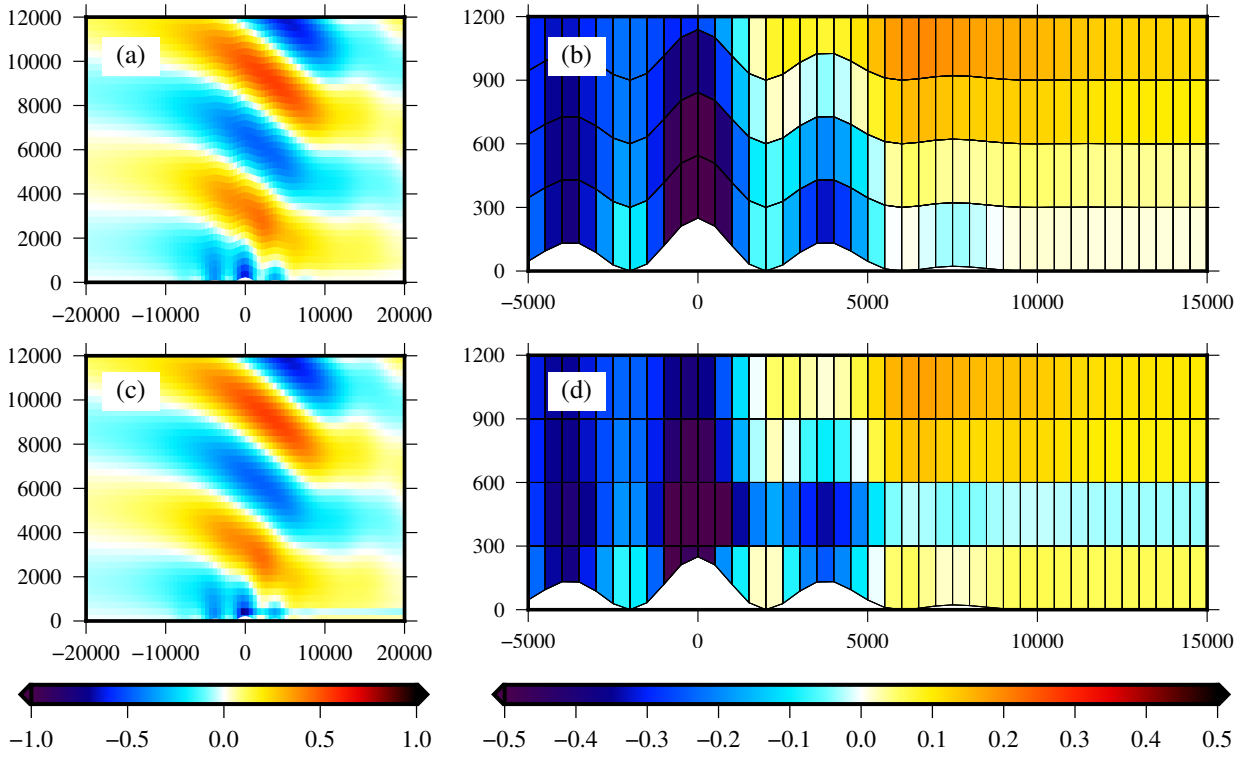

FIG. 5. Anomalies in potential temperature in the gravity waves test after 5 hours. The central domain in the lowest 12 km is shown on (a) the BTF grid, and (c) the cut cell grid. The four lowest layers of each grid are shown for (b) BTF, and (d) cut cell grids, using a narrower potential temperature scale.

- SnapCol w two orders of magnitude smaller in resting atmosphere test
- SnapCol advection test as good as noOrography

With the exception of the Lorenz computational mode on the SnapCol grid in the gravity waves test, results were satisfactory across BTF, SLEVE and SnapCol grids in all three test cases.

Miscellany:

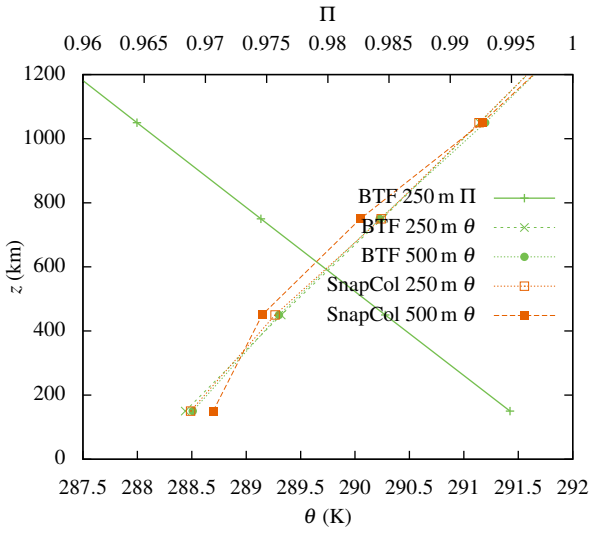

FIG. 6. Vertical profiles of the Exner function of pressure, Π, and potential temperature, θ, in the gravity waves test. Exner profile is visually identical on all grids for both mountain heights; for clarity, the Exner profile is only plotted for the BTF grid. The computational mode is manifested as a zig-zag in potential temperature on the cut cell grid which. Doubling the mountain height from 250 m to 500 m increases the severity of the computational mode but has negligible effect on the BTF grid. Results on the SLEVE grid (not shown) are qualitatively the same as those on the BTF grid for both mountain heights.

- Advection accuracy depends on alignment of the flow with grid layers (TODO: *we kinda need wobblyTracerAdvection to reach this conclusion*)

5. Further work

- Lorenz computational mode motivates formulation of C-P staggering for cut cell grids
- Find out what excites the Lorenz computational mode
- TODO: *anything else?*

Acknowledgments. Start acknowledgments here.

References

Dempsey, D., and C. Davis, 1998: Error analyses and test of pressure gradient force schemes in nonhydrostatic, mesoscale model. Preprints, *12th Conf. on Numerical Weather Prediction*, Phoenix, AZ, 236–239.

Gal-Chen, T., and R. C. Somerville, 1975: On the use of a coordinate transformation for the solution of the navier-stokes equations. *J. Comp. Phys.*, **17**, 209–228.

Good, B., A. Gadian, S.-J. Lock, and A. Ross, 2014: Performance of the cut-cell method of representing orography in idealized simulations. *Atmos. Sci. Lett.*, **15**, 44–49.

Jebens, S., O. Knoth, and R. Weiner, 2011: Partially implicit peer methods for the compressible euler equations. *J. Comp. Phys.*, **230**, 4955–4974.

Klein, R., K. Bates, and N. Nikiforakis, 2009: Well-balanced compressible cut-cell simulation of atmospheric flow. *Philos. Trans. Roy. Soc. London*, **367**, 4559–4575.

Klemp, J. B., 2011: A terrain-following coordinate with smoothed coordinate surfaces. *Mon. Wea. Rev.*, **139**, 2163–2169.

Leuenberger, D., M. Koller, O. Fuhrer, and C. Schär, 2010: A generalization of the SLEVE vertical coordinate. *Mon. Wea. Rev.*, **138**, 3683–3689.

Melvin, T., M. Dubal, N. Wood, A. Staniforth, and M. Zerroukat, 2010: An inherently mass-conserving iterative semi-implicit semi-lagrangian discretization of the non-hydrostatic vertical-slice equations. *Quart. J. Roy. Meteor. Soc.*, **136**, 799–814.

Phillips, N. A., 1957: A coordinate system having some special advantages for numerical forecasting. *J. Meteor.*, **14**, 184–185.

Schär, C., D. Leuenberger, O. Fuhrer, D. Lüthi, and C. Girard, 2002: A new terrain-following vertical coordinate formulation for atmospheric prediction models. *Mon. Wea. Rev.*, **130**, 2459–2480.

Steppeler, J., H.-W. Bitzer, M. Minotte, and L. Bonaventura, 2002: Nonhydrostatic atmospheric modeling using a z-coordinate representation. *Mon. Wea. Rev.*, **130**, 2143–2149.

Steppeler, J., and Coauthors, 2006: Prediction of clouds and rain using a z-coordinate nonhydrostatic model. *Mon. Wea. Rev.*, **134**, 3625–3643.

Weller, H., and A. Shahrokhi, 2014: Curl free pressure gradients over orography in a solution of the fully compressible euler equations with implicit treatment of acoustic and gravity waves. *Mon. Wea. Rev.*, **142**, 4439–4457.

Yamazaki, H., and T. Satomura, 2010: Nonhydrostatic atmospheric modeling using a combined cartesian grid. *Mon. Wea. Rev.*, **138**, 3932–3945.

Zängl, G., 2012: Extending the numerical stability limit of terrain-following coordinate models over steep slopes. *Mon. Wea. Rev.*, **140**, 3722–3733.